

HYDROGENATED AMORPHOUS SILICON CARBIDE AS A WINDOW MATERIAL FOR HIGH EFFICIENCY a-Si SOLAR CELLS

Yoshihisa TAWADA*, Masataka KONDO,
Hiroaki OKAMOTO and Yoshihiro HAMAKAWA

*Faculty of Engineering Science, Osaka University,
Toyonaka, Osaka 560, Japan*

Received 16 November 1981

Properties and fabrication technical data on glow discharge produced hydrogenated amorphous silicon carbide have been described. A series of experimental studies of the effects of impurity doping on amorphous silicon carbide has also been carried out. It has been shown from the experiment that hydrogenated amorphous silicon carbide prepared by the plasma decomposition of $[\text{SiH}_{4(1-x)} + \text{CH}_{4(x)}]$ gas mixture has a good valency electron controllability. Employing the property of the valency controlled a-SiC:H as a wide gap window junction, a-SiC:H/a-Si:H heterojunction solar cells have been fabricated. As a result, we have succeeded in breaking through an 8% efficiency barrier with this new material. A typical performance of a-SiC:H/a-Si:H heterojunction cell is J_{sc} of 15.21 mA/cm², V_{oc} of 0.88 V, FF of 60.1%, and η of 8.04%.

1. Introduction

Since Carlson and Wronski first developed an amorphous silicon solar cell in 1976 [1], remarkable progress has been seen in both material science and fabrication technology [2]. As a result, the efficiency of a-Si solar cell has been sharply improved: announced conference records are 7.55% with a-SiC:H/a-Si:H heterojunction cells [3], 7.0% with inverted p-i-n cells [4] and 6.6% with a-Si:F:H MIS cells [5].

The p-i-n a-Si solar cell might provide better reproducibility as well as being amenable to mass production and design control when put into practical application [6]. However, the p-i-n cell has one deficiency, that is, a large ineffective optical absorption in the p-layer which has a narrow optical band gap with a high density of nonradiative recombination centers [7]. Because of this ineffective absorption in the p-layer, the short-circuit current density decreases with increasing p-layer thickness contrary to the increase of the open-circuit voltage. Therefore, there exists an optimum thickness of the p-layer in the p-i-n a-Si solar cell, that is, about 80 Å [9].

*On leave from Kanegafuchi Chemical Industry Co. Ltd., 1-2-80 Yoshida-cho, Hyogo-ku, Kobe 652, Japan.

The ineffective absorption in the p-layer can be estimated to be about 12% at a wavelength of 5000 Å even if the thickness of p-layer is only 80 Å. If the optical absorption coefficient of p-side window material can be reduced to less than 1/10 of that of a-Si:H, this ineffective absorption might become negligibly small and the incident photon flux into an i-layer would increase. Therefore, using a valency electron controllable wide gap material as the window side junction material, we can improve not only the short-circuit current density but also the open-circuit voltage by increasing the p-layer thickness.

Recently, we have found a good valency electron controllability in a hydrogenated amorphous silicon carbide(a-SiC:H) prepared by the plasma decomposition of $[\text{SiH}_{4(1-x)} + \text{CH}_{4(x)}]$ gas mixture [9-11]. An a-SiC:H was firstly reported by Anderson and Spear [12]. Since their work, structural and photoluminescence studies of a-SiC:H have been performed [13-15]. However, information on the effects of impurity doping on the basic properties of a-SiC:H have not been reported. This paper presents a series of experimental data on the optical, electrical and optoelectronic properties of a-SiC:H for the highly efficient a-Si solar cell. Utilizing this valency controllable a-SiC:H as the p-side window, a-SiC:H/a-Si:H heterojunction solar cells having an efficiency of more than 8% have been developed.

2. Preparation and characterization of a-SiC:H films

2.1. Preparation of a-SiC:H films

Films of a-SiC:H were prepared with the plasma decomposition system as described in fig. 1. An a-SiC:H film can be fabricated by glow discharge decomposition of silane and hydrocarbon gas mixture [12-15]. However, the structure and optoelectronic properties of a-SiC:H films are significantly dependent upon both carbon sources and deposition conditions. Therefore, we examined the deposition conditions, the structure and the optoelectronic properties of a-SiC:H films which used methane(CH_4) and ethylene(C_2H_4) as carbon sources. The a-SiC:H film which used

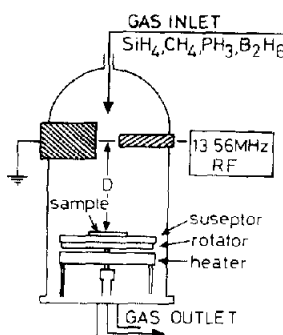


Fig. 1. Schematic diagram of the plasma reaction chamber.

Table 1
Deposition condition

SiH ₄	10% in H ₂
CH ₄	10% in H ₂
B ₂ H ₆ , PH ₃	500 ppm, 1000 ppm in H ₂
Pressure	2.3 Torr
Total flow	100 sccm
RF power	35 W
T _{sub}	250°C

C₂H₄ contains predominately Si—C₂H₅. On the other hand, in the a-SiC:H film which used CH₄, the Si—CH₃ bond is weakly present and other carbon atoms are incorporated as tetrahedral carbon in the amorphous Si network. On the other hand, from the view point of optoelectronic properties the a-SiC:H films which used CH₄ are superior to the a-SiC:H films which used C₂H₄. From these results, we adopted methane(CH₄) as a carbon source instead of ethylene(C₂H₄) as used by Anderson and Spear [12]. Furthermore, we optimized the deposition condition of boron doped a-SiC:H to promote tetrahedral bonding of carbon in a-SiC:H. The conditions of D=10 cm and rf power=35 W were chosen for the deposition of a-SiC:H. The detailed results will be reported in a separate paper in the near future. a-SiC:H films were deposited by the decomposition of [SiH_{4(1-x)} + CH_{4(x)}] on Corning #7059 glass for electrical, optical and optoelectronic measurements, and on high resistivity c-Si for IR spectrum measurement. The deposition conditions are shown in table 1.

2.2. Optical and photoconductive properties of a-SiC:H

The optical band gap $E_{g(opt)}$ of a-SiC:H films was determined from the straight line intercept of $(\alpha\hbar\omega)^{-1/2}$ versus $\hbar\omega$ curve at high absorption region ($\alpha > 10^4/\text{cm}$) following the analysis of Davis and Mott [16]. It seems unreasonable to measure the photoconductivity of a-SiC:H having a different optical band gap ranging from 1.76 to 2.2 eV under the same monochromatic illumination. Therefore, for various compositions of a-SiC:H, photoconductivity was measured under AM-1 (100 mW/cm²) illumination and under monochromatic illumination at which a-SiC:H has 10⁴/cm optical absorption coefficient. The monochromatic photoconductivity was normalized to $\eta\mu\tau$ proposed by Zanzucchi et al. [17]. Fig. 2 shows the photoconductivity σ_{ph} under AM-1 illumination versus the normalized photoconductivity $\eta\mu\tau$ for various compositions of a-SiC:H which have optical band gaps from 1.76 to 2.2 eV. As is seen in this figure, there exists an obvious relation between AM-1 photoconductivity and normalized photoconductivity. From these results, it is recognized that AM-1 photoconductivity can be commonly used as a quick judging method for optoelectronic properties of a-SiC:H having a different optical band gap energy from 1.76 to 2.2 eV.

Fig. 3 shows the gaseous compositional dependence of the optical band gap $E_{g(opt)}$ and AM-1 photoconductivity σ_{ph} of a-SiC:H. The optical band gap of undoped and boron doped a-SiC:H increases with increasing methane fraction of (x), but

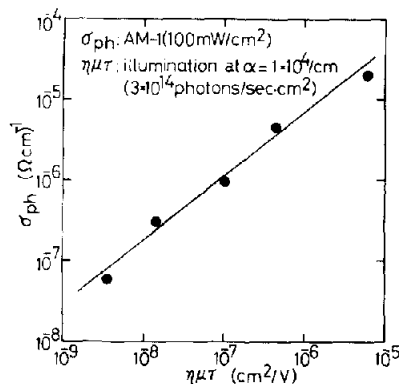


Fig. 2. AM-1 photoconductivity σ_{ph} versus normalized photoconductivity $\eta\mu\tau$ for various compositional a-SiC:H films.

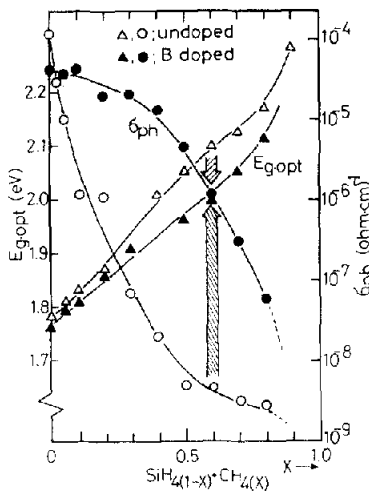


Fig. 3. Optical band gap $E_{g(opt)}$ and AM-1 photoconductivity σ_{ph} of undoped and boron doped a-SiC:H films.

the AM-1 photoconductivity of undoped material significantly decreases by adding a small amount of methane. On the other hand, boron doped material shows one to four orders of magnitude larger photoconductivity compared with undoped material. These improved photoconductivities of boron doped a-SiC:H are worth noting.

2.3. IR spectra of *a*-SiC:H

Fig. 4 shows the Si-H stretching mode absorptions of a-SiC:H deposited at $T_s = 250^\circ\text{C}$. As can be seen from this figure, the IR absorption coefficient of the 2000 cm^{-1} band decreases and the IR absorption coefficient of the 2090 cm^{-1} band increases with the increase of methane fraction of (x). Comparing this IR spectra with the significant photoconductivity decrease of undoped a-SiC:H as shown in fig. 3, there

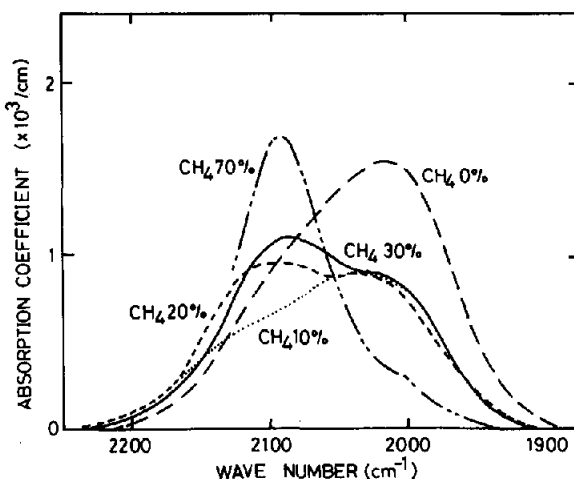
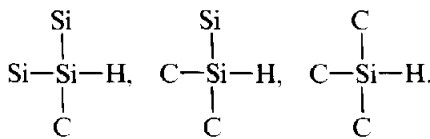


Fig. 4. IR stretching mode absorption of a-SiC:H films deposited at the substrate temperature of 250°C.

might be a close relationship between the increase of 2090 cm^{-1} band and the decrease of photoconductivity in undoped a-SiC:H. Wieder et al. [18] identified the 2090 cm^{-1} band as arising from the vibrational stretch of monohydride Si—H bonds attached with one, two or three carbons, respectively,



It may be possible that the decrease of photoconductivity in undoped a-SiC:H is caused by monohydride Si—H bonds attached with carbons.

2.4. Effects of impurity doping on the basic properties of a-SiC:H

Fig. 5 shows a summary of the effects of impurity doping on the basic properties of a-SiC:H prepared by the plasma decomposition of $[\text{SiH}_{4(0.8)} + \text{CH}_{4(0.2)}]$. As is seen in this figure, the dark conductivity σ_d at room temperature is of the order of $10^{-4} (\Omega\text{cm})^{-1}$ for 5% diborane doping and of the order of $10^{-2} (\Omega\text{cm})^{-1}$ for 0.1% phosphine doping. In contrast with these, the dark conductivity of undoped a-SiC:H is of the order of $10^{-10} (\Omega\text{cm})^{-1}$. The activation energy ΔE clearly changes from 1.08 eV for undoped a-SiC:H to 0.4 eV for diborane doping and to 0.2 eV for phosphine doping. So far as ascertained in terms of electrical conductivity and thermoelectric power measurement, p-n control is well achieved. The optical band gap $E_{\text{g}(\text{opt})}$ of doped a-SiC:H is almost constant except for sufficiently high boron doping.

Fig. 6 shows the effects of doping on the basic properties of a-SiC:H produced by decomposition of $[\text{SiH}_{4(0.5)} + \text{CH}_{4(0.5)}]$ gas mixture. A clear valency electron controllability can be also seen even in this case. The dark conductivity σ_d is on the order of $10^{-5} (\Omega\text{cm})^{-1}$ for 1% diborane doping and on the order of $10^{-3} (\Omega\text{cm})^{-1}$

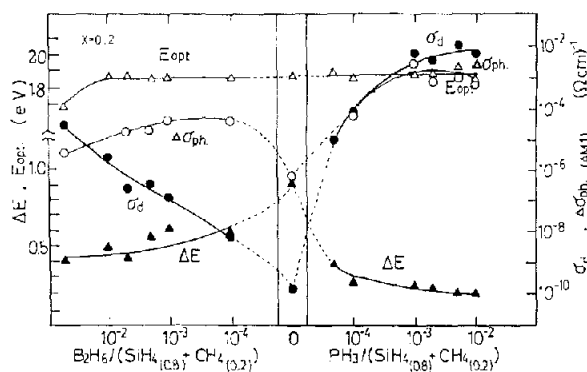


Fig. 5. Effects of impurity doping on the basic properties of a-SiC:H films prepared by the plasma decomposition of $[SiH_4(0.8) + CH_4(0.2)]$.

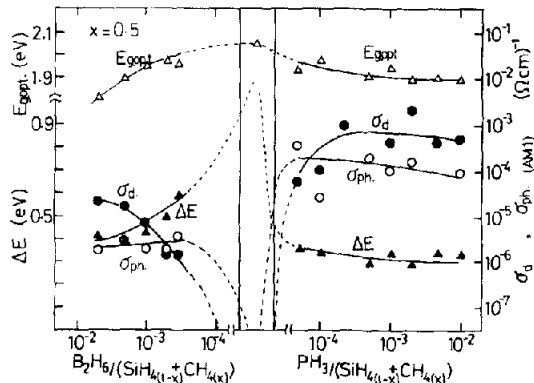


Fig. 6. Effects of impurity doping on the basic properties of a-SiC:H films prepared by the plasma decomposition of $[SiH_4(0.5) + CH_4(0.5)]$.

for 0.2% phosphine doping. The dark conductivity of undoped a-SiC:H is too small to measure at room temperature. The minimum activation energy is 0.4 and 0.3 eV for p- and n-type, respectively. In this case, the photoconductivity recovery by doping is remarkable, but the photoconductivity is one order smaller than the case of $x=0.2$. Optical band gap in this case is influenced by the impurity doping and decreases with the increase of doping fraction for both boron and phosphorus doping.

As can be seen in these data, a-SiC:H prepared by the plasma decomposition of $[SiH_4(1-x) + CH_4(x)]$ gas mixture can be effectively doped and might become a very useful window material for both a p-layer in the p-i-n structure and a n-layer in the inverted p-i-n cell structure.

3. a-SiC:H heterojunction solar cell and their properties

3.1. Fabrication of glass/SnO₂/p a-SiC:H/i-n a-Si:H/Al heterojunction solar cells

Various types of junction structures are now being investigated all over the world [19]. We have paid attention particularly to the junction structure of the p-i-n heteroface type [20] with a view to better process controllability and reproducibility for low cost solar cell production in the future. There are two types of p-i-n heteroface solar cell. One is glass/ITO(SnO₂)/p-i-n/metal and another one is ITO/p-i-n/metal substrate. In the present experiment, the glass/SnO₂/p-i-n/Al structure was employed because the fluctuation of series resistance originating in a transparent electrode in a solar cell was successfully suppressed. The substrate temperature during deposition was 250°C. A boron doped a-SiC:H layer of 100 Å was deposited on the substrate. Then an undoped a-Si:H of 5000 Å and a phosphorus doped a-Si:H of 500 Å were successively deposited. An aluminum electrode was evaporated onto the surface of an n-layer as a back side contact.

It is widely accepted that the properties of a-Si:H films are strongly influenced by rf power [21, 22]. Therefore, we optimized the deposition condition of undoped and phosphorous doped a-Si:H [9] in the p-i-n a-Si:H heteroface solar cell. One of the noticeable merits of our reaction system is that we can control the relative position *D* of the substrate to the discharge plasma while the energy density of the plasma can be controlled by adjusting the position of the rf coupling electrodes set outside the reaction chamber perpendicularly to the substrate as shown in fig. 1.

To the extent of this experiment concerning the undoped a-Si:H layer optimization in our deposition system, the most favorable condition for solar cell fabrication is *D* of 10 cm and rf power of 35 W [20]. Therefore, the conditions of *D*=10 cm and rf power of 35 W were chosen for the deposition of the undoped a-Si:H layer in a-SiC:H/a-Si:H heterojunction cells.

We examined the basic properties of phosphorus doped a-Si:H (PH₃/SiH₄=0.5 mol%) as a function of rf power for the electrode position *D* of 12.5 cm, as shown in fig. 7. As is seen in this figure, the dark conductivity increases exponentially and the activation energy decreases with increasing rf power in the region of more than 60 W. A crystalline structure was observed by the X-ray diffraction patterns in a phosphorous doped a-Si:H decomposed by more than 150 W rf power. A high conductive n-layer is favorable to reduce the series resistance of solar cells, but a higher rf power deposition might bring about impurity inclusion and also bombardment effects on the film. Therefore, we deposited phosphorous doped a-Si:H in the a-SiC:H/a-Si:H heterojunction solar cell under the condition of rf power=150 W and *D*=12.5 cm.

The sensitive area of solar cell is 3.3 mm² which was carefully evaluated to be about 5% larger than the deposited area of aluminum bottom electrode (area=3.14 mm²) by taking account of the experimentally confirmed edge effect to the photocurrent. *J-V* characteristics measurements were carried out under an AM-1 solar simulator. The solar simulator was calibrated by the standard a-Si solar cell. The performance of this standard cell was measured under sun light (near AM-1 sun light, at Toyonaka,

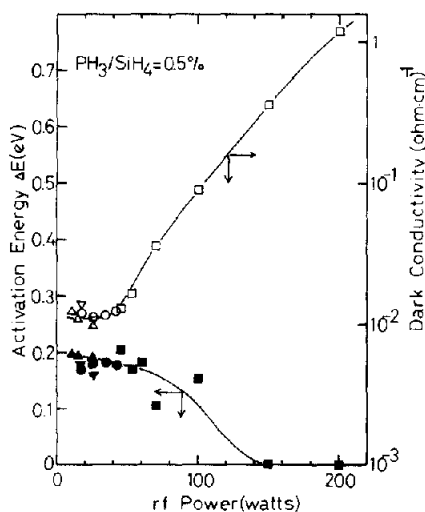


Fig. 7. Basic properties of phosphorus doped a-SiC:H films ($\text{PH}_3/\text{SiH}_4 = 0.5 \text{ mol\%}$) as a function of rf power for electrode position $D = 12.5 \text{ cm}$.

Osaka, Japan, July 1980). At this time, the solar radiation energy was measured by a NASA-calibrated c-Si solar cell and a pyroheliometer.

3.2. Basic properties of a-SiC:H in a-SiC:H/a-Si:H heterojunction solar cell

Hydrogenated amorphous silicon carbide showed not only a photoconductivity recovery effect by doping but also a valency electron controllability for both donors and acceptors. In the p-i-n cell structure, the activation energy ΔE and the dark conductivity σ_d of the p-layer are generally required to be less than 0.6 eV and more than $10^{-7} (\Omega\text{cm})^{-1}$, respectively. Therefore, p-type a-SiC:H having a wide band gap

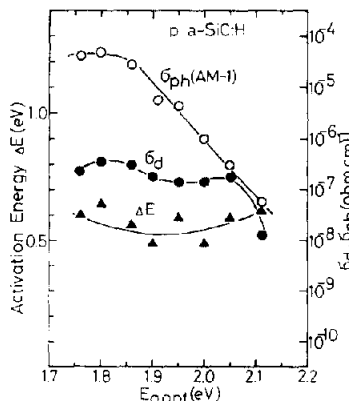


Fig. 8. Basic properties of boron doped a-SiC:H films as a function of optical band gap E_{gopt} .

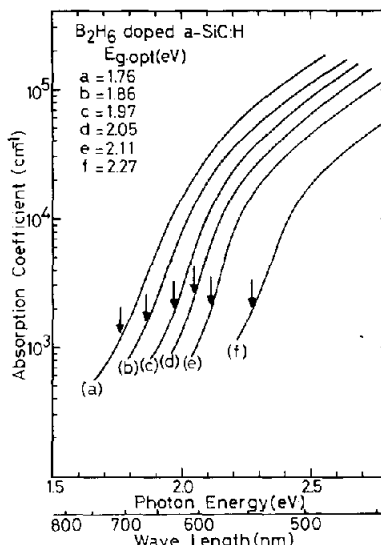


Fig. 9. Optical absorption spectra of boron doped a-SiC:H films as a parameter of optical band gap $E_{g(\text{opt})}$

ranging from 1.8 to 2.1 eV was utilized in the solar cell construction. The activation energy ΔE and the dark conductivity σ_d of these a-SiC:H films were about 0.55 eV and on the order of $10^{-7} (\Omega\text{cm})^{-1}$, respectively as shown in fig. 8.

Fig. 9 shows the optical absorption spectra of these a-SiC:H alloys as a function of wavelength. As is seen in this figure, the optical absorption spectra of these materials shift to higher energy region as compared with a-Si:H. An essential matter required for high efficiency a-Si solar cell is to effectively introduce the incident photons into the i-layer where the photocurrent is mainly produced. The ineffective absorption in the window side p-layer having an optical band gap of more than 2 eV for the p-i-n junction cell is negligibly small; on the other hand, there might be about 12% ineffective absorption in a p-layer of a p-i-n a-Si:H solar cell. Utilizing a-SiC:H as a p-side window material, we have fabricated a-SiC:H/a-Si:H heterojunction solar cells.

3.3. Photovoltaic performances of a-SiC:H/a-Si:H heterojunction solar cells as a function of the optical band gap of p-type a-SiC:H

Fig. 10 shows the photovoltaic performances of a-SiC:H/a-Si:H heterojunction solar cells as a function of the optical band gap $E_{g(\text{opt})}$ of p-type a-SiC:H. As is seen in this figure, not only the short-circuit current density J_{sc} but also the open-circuit voltage V_{oc} increases with increasing the optical band gap $E_{g(\text{opt})}$ of the p-layer. The short-circuit current density J_{sc} increases from 10.5 mA/cm² for an $E_{g(\text{opt})}$ of 1.76 eV that is p-type a-Si:H, to more than 12.4 mA/cm² for an $E_{g(\text{opt})}$ of 2.05 eV and shows a tendency to saturate for an $E_{g(\text{opt})}$ of more than 2 eV. The open-circuit voltage V_{oc} also increases from 0.80 to 0.91 V as the increase of $E_{g(\text{opt})}$ of p-layer from 1.76 to 2.11 eV. The fill factor FF is almost constant except for $E_{g(\text{opt})}$ of more than 2.1 eV. To the extent of the present experiments concerning boron doped a-SiC:H having $E_{g(\text{opt})}$ of

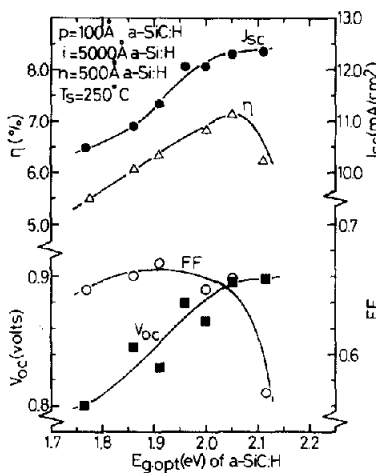


Fig. 10. Photovoltaic performances of a-SiC:H/a-Si:H heterojunction solar cells as a function of optical band gap $E_{g(\text{opt})}$ of window side p-layer.

more than 2.2 eV, it is difficult to control its valency electron. Therefore, there exists an optimum $E_{g(\text{opt})}$ of the p-layer, that is, about 2 eV at the present stage. If we could control the valency electron of a-SiC:H having an $E_{g(\text{opt})}$ of more than 2.2 eV, it might be possible to make this optimum $E_{g(\text{opt})}$ larger.

3.4. Effects of p-type a-SiC:H on the short-circuit current density J_{sc} and the open-circuit voltage V_{oc}

a-SiC:H/a-Si:H heterojunction solar cells show not only larger J_{sc} but also larger V_{oc} than the ordinary p-i-n a-Si:H homojunction solar cells. More direct experimental evidence can be seen in the collection efficiency data as shown in fig. 11. As is seen in this figure, the collection efficiency of these heterojunction cells is extremely improved especially near the peak of the solar energy spectrum with increasing $E_{g(\text{opt})}$ of the p-layer. These improvements are caused by a wide gap window effect of the p-layer and also by the enhancement of the internal electric field caused from the larger potential difference at the p-i interface. The former results in the reduction of the optical loss in the p-layer and the latter increases the carrier collection efficiency.

As for effects of a-SiC:H on the open-circuit voltage V_{oc} , there exists a clear correlation between the open-circuit voltage V_{oc} and the diffusion potential V_d in a p-i-n junction, as shown in fig. 12. The p-type a-SiC:H can increase the diffusion potential of a p-i-n junction and 1/3 part of the increased diffusion potential contributes to the increase of the open-circuit voltage V_{oc} . This result shows us that it might be possible to obtain a larger open-circuit voltage by optimization of p-type a-SiC:H. These experimental facts imply that not only a wide gap window effect, but also a voltage factor due to the potential profile steepened with a wide gap a-SiC:H contribute to the improvement of the photovoltaic performances of a-SiC:H/a-Si:H heterojunction solar cell.

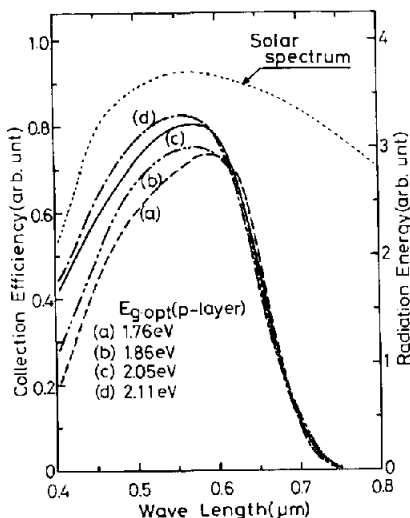


Fig. 11. Collection efficiency spectra of a-SiC:H/a-Si:H heterojunction solar cells as a parameter of optical band gap $E_{g(\text{opt})}$ of window side p-layer.

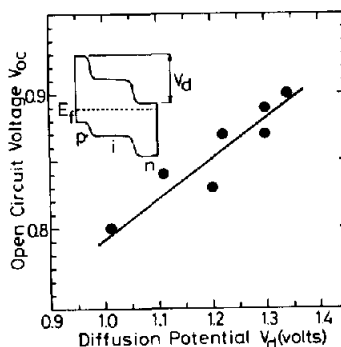


Fig. 12. Correlation between the open-circuit voltage V_{oc} and the diffusion potential V_d in a-SiC:H/a-Si:H heterojunction solar cells.

3.5. Photovoltaic performances dependence on the thickness of p-type a-SiC:H

It is well known that the open-circuit voltage V_{oc} and the short-circuit current density J_{sc} strongly depend upon the thickness of a p-layer in a p-i-n a-Si solar cell [7]. This dependency is caused by a homogeneity and a large optical absorption of a p-type a-SiC:H. The a-SiC:H film has a larger optical band gap than the a-Si:H film so that the photovoltaic performance dependence on the thickness of p-type a-SiC:H may be different from the case of p-type a-Si:H. Fig. 13 shows the photovoltaic performance dependence on the thickness of the p-layer having an $E_{g(\text{opt})}$ of 2.05 eV. The short-circuit current density J_{sc} increases with increasing thickness up to about 100 Å, and does not exhibit any change even though the p-layer thickness

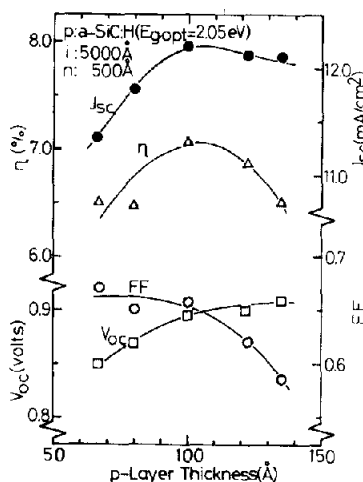


Fig. 13. Photovoltaic performances of a-SiC:H/a-Si:H heterojunction solar cells as a function of the thickness of the p-layer with an $E_{g(opt)}$ of 2.05 eV.

is more than 100 Å. It is because the optical absorption of this p-layer is so small that the ineffective absorption is almost negligible. The open-circuit voltage V_{oc} increases up to 0.91 V with increasing p-layer thickness. However, the increase of the p-layer thickness reduces the fill factor FF owing to the effect of series resistance involved in a p-layer. Therefore, the optimum layer thickness of the p-layer is 100 Å.

4. Typical $J-V$ characteristics of a-SiC:H/a-Si:H heterojunction solar cells

Through further optimizations of film quality and cell parameters, the conversion efficiency of an a-SiC:H/a-Si:H heterojunction solar cell has been improved to 7.82%. While, an ordinary p-i-n a-Si:H homojunction solar cell showed the conversion efficiency of 5.7%. Fig. 14 shows $J-V$ characteristics of this a-SiC:H/a-Si:H heterojunction solar cell and an ordinary p-i-n a-Si:H homojunction solar cell for comparison. The performance of an a-SiC:H/a-Si:H heterojunction solar cell is $\eta = 7.82\%$, $V_{oc} = 0.903$ V, $J_{sc} = 13.76$ mA/cm² and FF = 62.9%. On the other hand, the conversion efficiency of an ordinary p-i-n a-Si:H solar cell is 5.7% with V_{oc} of 0.801 V, J_{sc} of 11.02 mA/cm² and FF of 64.7%. As is seen in these data, the performance of an a-SiC:H/a-Si:H heterojunction solar cell is clearly improved by 24.9% in J_{sc} , 13.7% in V_{oc} , and 37% in η as compared with an ordinary p-i-n a-Si:H homojunction solar cell. These remarkable improvements of J_{sc} and V_{oc} are caused by the wide band gap effects of a-SiC:H, that is, the decrease of ineffective absorption in the p-layer and the increase of the diffusion potential in the p-i-n junction. The sensitive area of these cells is 3.3 mm². As for a large area solar cell (1.0 cm²), the conversion efficiency of 7.72% has been obtained with $J_{sc} = 14.06$ mA/cm², $V_{oc} = 0.880$ V and FF = 62.4% with glass/ITO/SnO₂ substrate as shown in fig. 15.

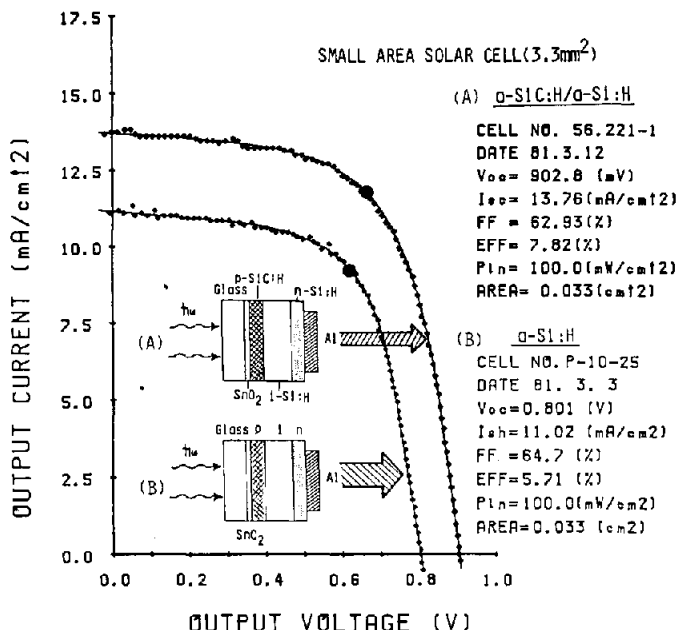


Fig. 14. Photovoltaic performances of an a-SiC:H/a-Si:H heterojunction solar cell (A) and an a-Si:H p-i-n homojunction solar cell (B) with glass/SnO₂ substrate. (A) $J_{sc}=13.76\text{ mA/cm}^2$, $V_{oc}=0.903\text{ V}$, FF = 62.9%, $\eta=7.82\%$. (B) $J_{sc}=11.02\text{ mA/cm}^2$, $V_{oc}=0.801\text{ V}$, FF = 64.7%, $\eta=5.71\%$. Area = 3.3 mm², $P_{in}=100\text{ mW/cm}^2$.

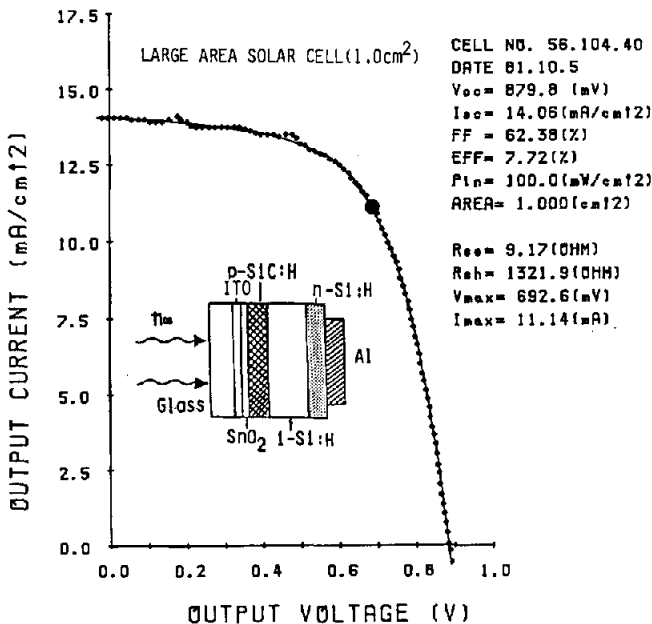


Fig. 15. Photovoltaic performance of a large area a-SiC:H/a-Si:H heterojunction solar cell. $J_{sc}=14.06\text{ mA/cm}^2$, $V_{oc}=0.880\text{ V}$, FF = 62.4%. $\eta=7.72\%$. Area = 1.0 cm², $P_{in}=100\text{ mW/cm}^2$.

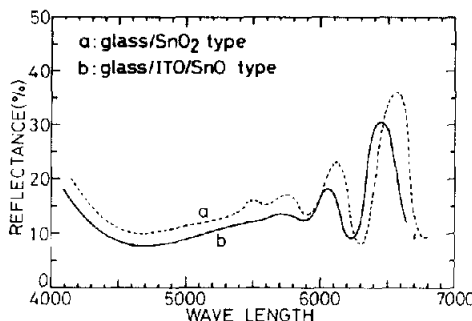


Fig. 16. Typical reflection spectrum of glass/SnO₂ type solar cell.

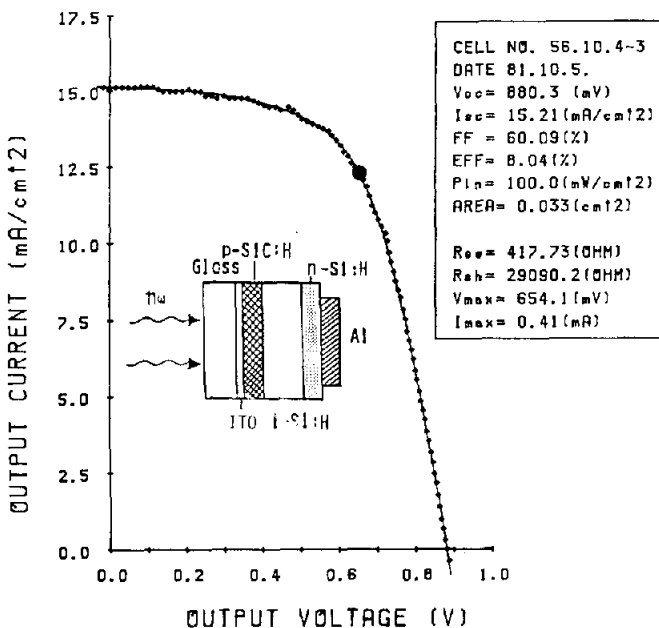


Fig. 17. The highest photovoltaic performance of an a-SiC:H/a-Si:H heterojunction solar cell with glass/antireflective ITO substrate. $J_{sc} = 15.21 \text{ mA/cm}^2$, $V_{oc} = 0.880 \text{ V}$, FF = 60.1%, $\eta = 8.04\%$. Area = 3.3 mm², $P_{in} = 100 \text{ mW/cm}^2$.

Fig. 16 shows the reflection spectra of these solar cells. As is seen in this figure, the loss by reflection can be estimated to be from 12 to 15%. This can be reduced to less than 5% by the optimization of the thickness of ITO; then more than 8% conversion efficiency has been obtained with the a-SiC:H/a-Si:H heterojunction solar cell structure as shown in fig. 17. The performance of this cell is J_{sc} of 15.21 mA/cm², V_{oc} of 0.88 V, FF of 60.1% and η of 8.04%.

Furthermore, the best short-circuit current density, open-circuit voltage and fill factor separately observed in a-SiC:H/a-Si:H heterojunction solar cells are 15.21

mA/cm^2 , 0.91 V and 0.71, respectively. Therefore, the efficiency of 9.8% might be realistically obtained in a near future with a-SiC:H/a-Si:H heterojunction structure.

5. Discussion and summary

We have conducted a series of experimental investigations on the optical, electrical and optoelectronic properties of a-SiC:H prepared by the plasma decomposition of $[\text{SiH}_{4(1-x)} + \text{CH}_{4(x)}]$ and also on the usefulness of a-SiC:H in a-SiC:H/a-Si:H heterojunction solar cells. The photoconductivity of an undoped a-SiC:H sharply decreases with increasing methane fraction, but boron doped a-SiC:H shows one to three orders of magnitude larger photoconductivity as compared with undoped material. From the investigation of the IR spectra, the decrease of photoconductivity in an undoped a-SiC:H correlates with monohydride Si-H bonds attached with carbons. The results of impurity doping on a-SiC:H imply that there is good doping efficiency for both donors and acceptors. Furthermore, a doped a-SiC:H has a large optical band gap which can be controllable by methane fraction. So far as ascertained in terms of electrical conductivity and thermoelectric power measurements, p-n control is well achieved in a-SiC:H having $E_{\text{g(opt)}}$ from 1.8 to 2.1 eV. The p-i-n cell has a deficiency which results from a large ineffective optical absorption in the p-layer. This ineffective absorption can be estimated to be about 12% at a wavelength of 5000 Å even if the thickness of the p-layer is only 80 Å. Utilizing a valency electron controllable wide gap material having $E_{\text{g(opt)}}$ of more than 2 eV as a window side doped layer, this ineffective absorption is made negligible and the incident photon flux into the i-layer increased. Therefore, these results show us that a-SiC:H is a very useful window material for both p-i-n and inverted p-i-n cell constructions. We investigated the effects of a-SiC:H in a-SiC:H/a-Si:H heterojunction solar cells. It is clear that not only J_{sc} but also V_{oc} of the a-SiC:H/a-Si:H heterojunction solar cell increases with increasing $E_{\text{g(opt)}}$ of a-SiC:H. The collection efficiency of these cells is extremely improved especially near the peak of the solar energy spectrum with increasing $E_{\text{g(opt)}}$ of the p-layer. These improvements are caused by the wide band gap effect of a-SiC:H. This is because an a-SiC:H reduces the ineffective absorption in a p-layer and increases the internal electric field in a p-i-n junction. As for the increase of V_{oc} , a clear relation can be seen between the open-circuit voltage V_{oc} and the diffusion potential V_d . From this linear relation, it is recognized that 1/3 of the increase of the diffusion potential contributes to the increase of the open-circuit voltage V_{oc} . This result shows that it might be possible to obtain a larger open-circuit voltage V_{oc} by the optimization of a-SiC:H. As for the optimum $E_{\text{g(opt)}}$ of p-layer, it can be estimated to be about 2 eV.

The conversion efficiency given by the further optimization with glass/SnO₂ substrate is 7.82% with J_{sc} of 13.76 mA/cm^2 , V_{oc} of 0.903 V and FF of 62.9%. Comparing this cell with an ordinary p-i-n a-Si:H homojunction solar cell, the performance of this a-SiC:H/a-Si:H heterojunction solar cell is clearly improved by 24.9% in J_{sc} , 12.7% in V_{oc} and 37% in η . As for a large area (1.0 cm^2) solar cell, 7.72% conversion efficiency has been obtained with J_{sc} of 14.1 mA/cm^2 , V_{oc} of 0.880 V and FF of 62.4%.

by using a glass/ITO/SnO₂ substrate. The loss by reflection of these cells was estimated to be from 12 to 15%. We can reduce this reflection to less than 5% by the optimization of ITO thickness. Therefore, more than 8% conversion efficiency has been obtained with glass/ITO/p a-SiC:H/i-n a-Si:H heterojunction structure. The performance of this cell is J_{sc} of 15.21 mA/cm², V_{oc} of 0.88 V, FF of 60.1% and η of 8.04%. This result shows that a-SiC:H is one of the most favorable window side junction materials. Furthermore, the best short-circuit current density, open-circuit voltage and fill factor separately observed in a-SiC:H/a-Si:H heterojunction solar cells are 15.21 mA/cm², 0.91 V and 71%, respectively. Therefore, an efficiency of 9.8% might be realistically obtained in the near future with an a-SiC:H/a-Si:H heterojunction structure. An additional noticeable merit in the proposed new solar cell is a very strong mechanical strength with chemical and thermal stabilities.

Acknowledgements

The authors wish to thank Prof. A. Hiraki and Dr. T. Imura of Osaka University and Mr. S. Kubo of Kanegafuchi Chemical Industry Co. Ltd. for helpful discussions. Technical assistance by Mr. C. Sada is also acknowledged. They also thank Messrs. K. Tsuge and K. Fujimoto for first response measurements. This work is partially supported by "Special Research Project on Amorphous Materials and Physics" sponsored by the Ministry of Education and "Sunshine Project, Solar Photovoltaic Division" sponsored by the Agency of Industrial Science and Technology.

References

- [1] D. E. Carlson and C. R. Wronski, *Appl. Phys. Lett.* 28 (1976) 671.
- [2] Y. Hamakawa, Proc. 9th Intern. Conf. on Amorphous and Liquid Semiconductors, Grenoble (1981) to be published.
- [3] Y. Tawada, M. Kondo, H. Okamoto and Y. Hamakawa, Proc. 15th IEEE Photovoltaic Specialists Conf., Florida (1981) p. 245.
- [4] Y. Uchida, T. Ichimura, M. Ueno and M. Ohsawa, Proc. 9th Intern. Conf. on Amorphous and Liquid Semiconductors, Grenoble (1981) to be published.
- [5] A. Madan, J. MacGill, J. Yang, W. Czubatjy and S. R. Ovshinsky, Proc. 9th Intern. Conf. on Amorphous and Liquid Semiconductors, Grenoble (1981) to be published.
- [6] H. Okamoto, Y. Nitta, T. Adachi and Y. Hamakawa, *Surface Sci.* 86 (1979) 486.
- [7] H. Okamoto, Y. Nitta, T. Yamaguchi and Y. Hamakawa, *Solar Energy Mater.* 2 (1980) 313.
- [8] Y. Hamakawa, H. Okamoto and Y. Nitta, Proc. 14th IEEE Photovoltaic Specialists Conf., San Diego (1980) p. 1074.
- [9] Y. Tawada, H. Okamoto and Y. Hamakawa, *Appl. Phys. Lett.* 39 (1981) 237.
- [10] Y. Tawada, M. Kondo, H. Okamoto and Y. Hamakawa, Proc. 9th Intern. Conf. on Amorphous and Liquid Semiconductors, Grenoble (1981) to be published.
- [11] Y. Tawada, M. Kondo, H. Okamoto and Y. Hamakawa, Proc. 13th Conf. on Solid State Devices, Tokyo (1981) to be published.
- [12] D. A. Anderson and W. E. Spear, *Phil. Mag.* 35 (1977) 1.
- [13] D. Engemann and R. Fischer, *Appl. Phys. Lett.* 32 (1978) 567.
- [14] A. Guivarc'h, J. Richard and M. Contellec, *J. Appl. Phys.* 51 (1980) 2167.

- [15] R. S. Sussmann and R. Ogden, *Phil. Mag. B* 44 (1981) 137.
- [16] E. A. Davis and N. F. Mott, *Phil. Mag.* 22 (1970) 903.
- [17] P. J. Zanzucchi, C. R. Wronski and D. E. Carlson, *J. Appl. Phys.* 48 (1977) 5227.
- [18] H. Wieder, M. Cardona and C. R. Guarneri, *Phys. Stat. Sol. (b)* 92 (1979) 99.
- [19] Y. Hamakawa, *Surface Sci.* 86 (1979) 444.
- [20] Y. Tawada, T. Yamaguchi, S. Nonomura, S. Hotta, H. Okamoto and Y. Hamakawa, *Japan. J. Appl. Phys.* 20 (1981) suppl. 20-2, 213.
- [21] J. C. Nights, *Japan. J. Appl. Phys.* 18 (1979) suppl. 18-1, 100. *Solids* 35/36 (1980) 475.
- [22] K. Tanaka, S. Yamasaki, A. Matsuda, H. Okushi, M. Matsumura and S. Iizima, *J. Non-Crystalline Solids* 35/36 (1980) 475.